Materials Science Forum Vols. 638-642 (2010) pp 769-774
Online available since 2010/Jan/12 at www.scientific.net

doi:10.4028/www.scientific.net/MSF.638-642.769

MICROSTRUCTURAL AND MECHANICAL CHARACTERIZATION OF GRAY CAST IRON AND AlSi ALLOY AFTER LASER BEAM HARDENING

W A Monteiro[1,2,a], E M R. Silva[2,b], L V Silva[1,c], W de Rossi[3,d], S J Buso[2]

[1] Physics Department, Sciences and Humanities Center, Presbyterian Mackenzie University, Rua da Consolação, 896, prédio 12, Consolação, CEP 01302-907, São Paulo - SP, Brazil

[2] CCTM – Institute of Energetic and Nuclear Researches (IPEN), São Paulo - SP, Brazil.

[3]CLA – Institute of Energetic and Nuclear Researches (IPEN), São Paulo - SP, Brazil.

[a] fisica.cch@mackenzie.br, [b] emsilva@ipen.br, [c] lu.ventavele@gmail.com, [d] wderossi@ipen.br

Keywords: Gray cast iron, Al-Si alloy, surface hardening treatment, Nd:YAG pulsed laser, characterization, electron microscopy.

Abstract. A localized source of heat, such as that of laser beam, can provide a convenient means of producing a surface layer of altered microstructure. By using surface hardening treatment, wear resistance can be increased. Experiments were performed using a Nd:YAG pulsed laser under different processing conditions. Scanning electron microscopy (SEM), energy dispersive spectroscopy (EDS) and X-ray mapping (SEM) were employed to observe the effect of laser melting treatment on the microstructural properties of the samples. Depending on the selected laser treatment working conditions, different microstructures characteristics of surface melting can be achieved in the treated zone. Higher microhardness values were found at the treated area showing a superficial hardening of the sample and, consequently, an improvement of the wear resistance of these automotive alloys. The aim of this work is to find the optimal process parameters and to evaluate the characteristics of the laser superficial hardening (LSH) in a pearlitic gray iron and Al-Si alloy used in an automobile industry (bearing and piston materials in automotive industry).

Introduction

Surface properties of materials are strongly involved in wear and failure mechanisms. Wear resistance of metals can be improved through an increased hardness of the surface. Thermochemical, mechanical, or thermal surface treatments of metallic materials have been investigated and some of them are currently used in the industry.

The high power lasers offer original solutions concerning treatments surface technology and present some advantages when compared with conventional heat treatment methods. The main advantages are: extremely high cooling rates, heating of localized areas without affecting the metal bulk, versatility and higher process velocity, leading to high efficiency [1].

Laser processing depends on set of variables of the laser source (wavelength, operation mode, power, laser beam diameter, etc.) and of the material (geometry, physical properties and laser absorption). If the process is to be useful in industry it is necessary to select, for a given material, their best combination of these parameters. Pulsed Nd:YAG lasers are versatile tools that have been used for heating metals efficiently and can be used with fiber optic beam delivery: these have made an impact in the field of more complex three-dimensional processing [1 - 3].

Materials and Methods

The first experimental study was performed with a pearlitic gray iron [4] used in an automobile engine. The chemical composition (wt %) is 91.7%Fe; 3.45%C; 2.4%Si; 0.65%P; 0.75%Mn;

0.66%Cu; 0.38%Cr. Figure 1 shows the morphological aspect and distribution of the graphite in this gray iron as received. Surface heat treatments have been applied to samples (40mm x10mm x 8mm) taken from an automotive cylinder.

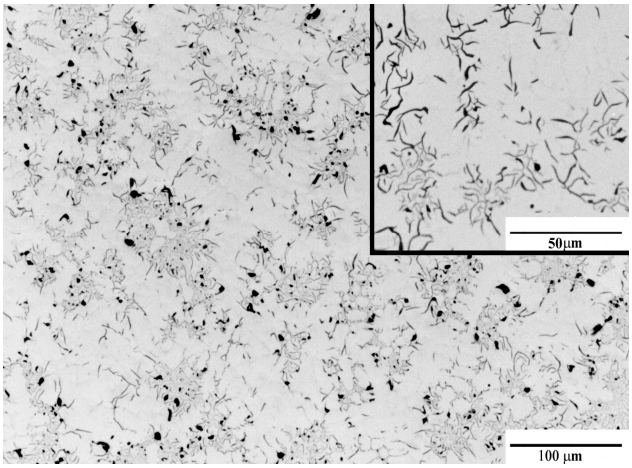

Fig.1 - Morphological pattern utilizing optical microscopy of graphite in the *gray cast iron*.

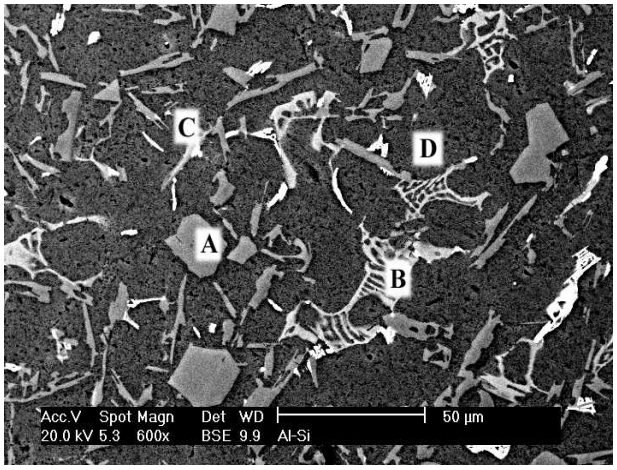

Fig.2 - SEM micrograph of as received *Al-Si alloy*; A: silicon particle; B: particle rich in Cu; C: eutectic rich in silicon; D: Matrix.

Table 1 Operating conditions of the tests for gray cast iron.

Processing Condition	L2	L5
(W_p) [kW/cm^2]	106	92
(τ) [ms]	10	10
ΔH [mm]	5.8	8.8
Track:		
O (%)	15	15
SV (mm/min)	542	384

Table 2 Operating Conditions of the Tests for cast Al-Si alloy.

Processing Condition	I	II	III
(W_p) [kW/cm^2]	236	145	139
(τ) [ms]	12.3	13.7	10
ΔH [mm]	4.8	2.8	4.8
Track			
O (%)	15	15	15
SV (mm/min)	328	386	471

The surface treatments were carried out using a pulsed Nd: YAG laser (λ = 1.06µm) with a beam multimode spatial distribution under argon protective atmosphere. The average absorption, A, for λ = 1.06µm in gray cast iron samples is 32.3 ± 2.0%. This value was obtained experimentally by calorimetric method [5]. Individual pulses and tracks of laser under different processing conditions were studied. Only the distance between focal plane and sample surface (ΔH) was modified to obtain variation of beam dimension. The processing parameters are presented in Table 1, where W_p is the Power Density, τ the Temporal Width, ϕ the Diameter of the melted pool, **O** the overlapping and **SV** the Scan Velocity. The results of laser treatment were analyzed by means of optical and scanning electron microscopy examination of transversal cross-sections of the treated zones. Vickers hardness (HV) was measured at different depths. The roughness measurements were performed by means of a Mitutoyo tester.

The second experimental study was performed with cast Al-12Si-1.5Cu (wt %) that was used as the substrate material. The figure 2, obtained by SEM, shows its morphological aspect in the as received condition. Cylindrical samples (12.7mm x 12 mm), taken from an Al-Si automotive piston, were superficially ground until 1000-mesh and cleaned with ethanol under ultrasonic vibration. The surface treatments were carried out using the same laser system as for the gray iron case. All tests were also performed under argon protective atmosphere. The average absorptivity, A, for Nd: YAG laser beam in Al-Si samples [5] is 5.2 ± 1.1%.

Individual pulses and tracks of laser under different processing conditions were studied. Again, only distance between focal plane and sample surface (ΔH) was modified to obtain variation of beam dimension. The processing parameters are presented in Table 2. Each treated surface of Al-Si alloy was etched with a solution of de HF-5% and analyzed macroscopically to verify the oxidation level and the possible changes of superficial roughness. After this, a microscopic exam of the cross area of each incident pulse using scanning electronic microscopy was done. It was evaluated possible modifications of the surface occurred in function of the different processing condition in this alloy. Vickers hardness (HV) was measured at different depths. The roughness measurements were also performed by means of a Mitutoyo tester.

RESULTS

Figures 3 and 4 correspond to a transverse section of the heat-affected zone after the surface laser treatment in gray cast iron with one individual pulse under condition L2 and L5, respectively. For individual pulses, the maximum depth (190μm), obtained in the central zone of the laser beam incidence, was found in condition L2-individual pulse. The maximal diameter, 880μm, was found in condition L5-individual pulse.

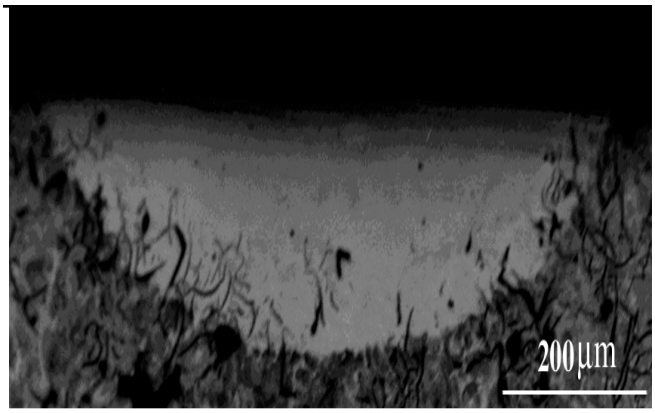

Fig.3 - Optical micrograph in *gray cast iron* showing typical cross-sectional structure of an individual laser pulse; Condition L2. Nital4%.

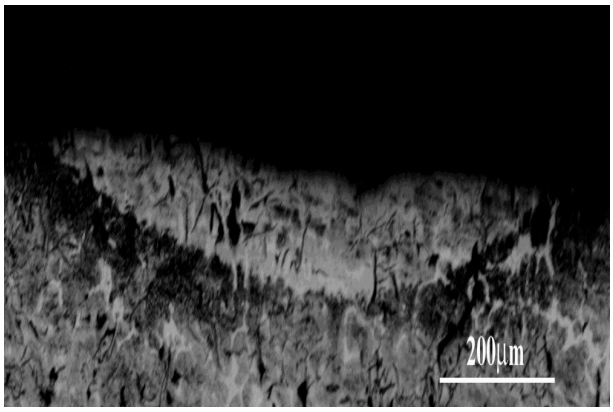

Fig.4 - Optical micrograph in *gray cast iron* showing typical cross-sectional structure of an individual laser pulse; Condition L5. Nital4%.

For all these experiments, it was verified that the microhardness increases with the decrease of the depth, because the carbon content of martensite increases with the depth. Values almost 300% higher than in the substrate one (240-260HV) were reached. Figures 5 and 6 correspond to a transverse section of the specimen (gray cast iron) with laser tracks under condition L2.
A little superficial roughness variation was established due to surface melting where a complete solubilization of the graphite lamellas was obtained. Some solidification cracks, caused by internal compression stress generated in the molten layer, associated with lamellar graphite could be observed. It was found regions with different aspects in affected area that are illustrated in Fig. 6. They are: (1) *Melt Zone* (MZ), (2) *Austenizatization Zone* (AZ), (3) *Unaffected Substrate* (US).
In condition L5-track, Figure 7, the pulses boundary is not clearly observed. This happens because only a hardened martensite surface layer without melted material evidence appears. In the hardened martensite zones the solubilization of the graphite lamellas was not completed. The microhardness was measured at a depth of 50μm and maximum values near 900HV were reached. The obtained hardness varies from 650 to 900HV, depending on the zone in the hardened layer.

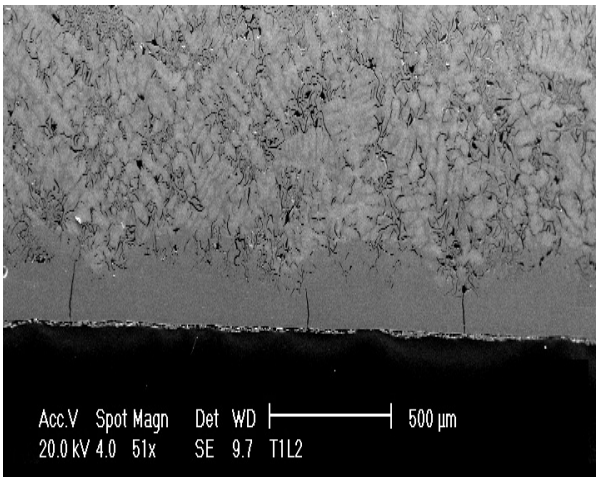

Fig.5 - SEM image of cross-section of *gray iron* sample with laser track; Condition L2-track. Nital 4%.

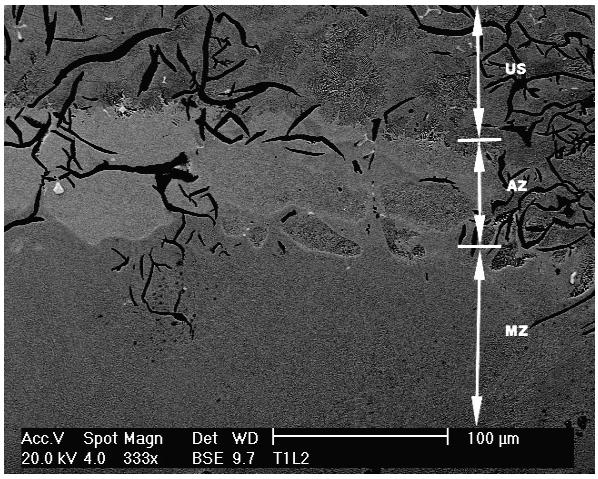

Fig.6 - SEM image of cross section of a single laser track in *gray cast iron*; Condition: L2-track. Nital 5% + Picral 4% + HCl.

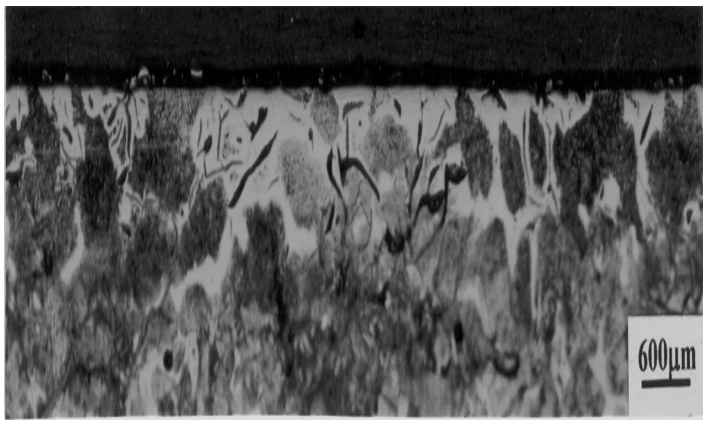

Fig. 7 - OM image of cross-section of *gray iron* sample with laser track; Condition L5. Nital 4%.

The scanning electron micrographs of the cross sections of Al-Si alloy of the individual laser pulses under the processing conditions, presented in Table 2, are illustrated in the figures below, where is possible to observe the boundary of the affected area. In the Figure 8 is presented a uniform affected area under condition I, where there was a complete dissolution and dispersion of the particles of Si and intermetallics.

In the condition II, the irradiated area presented the same characteristics to the condition I, but eventually, the remelting promotes the appearance of a region of dendritic cellular structure, developed during the solidification processing, as is illustrated in Figure 9. In condition III, figure 10, it is possible to observe the boundary of the area affected with some regions brighter than others, indicating its non homogeneity. The micrograph of a cross section of a laser track (condition II) is presented in Figure 11. The superficial roughness variation was insignificant.

With the laser remelting, it was achieved the decrease and more dispersion of the silicon particles. Through the rapid solidification, the silicon, elementary or eutectic, tends to the spheroidization. The particles tend to round off and, after dissolution, precipitate as fine particles. Thus, there is the microstructure refinement. In all condition, it was obtained a microhardness increase, reaching maximum values of 190HV for condition I, 200HV for condition II and 325HV for condition III, while the average microhardness of the substrate is 128 HV. The higher values of microhardness were found at the brighter areas.

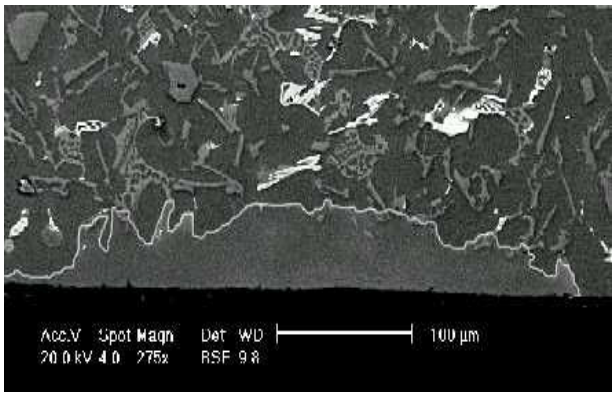

Fig.8 - SEM image of *Al-Si alloy* showing typical cross-sectional structure of an individual laser pulse; Condition: I-individual pulse.

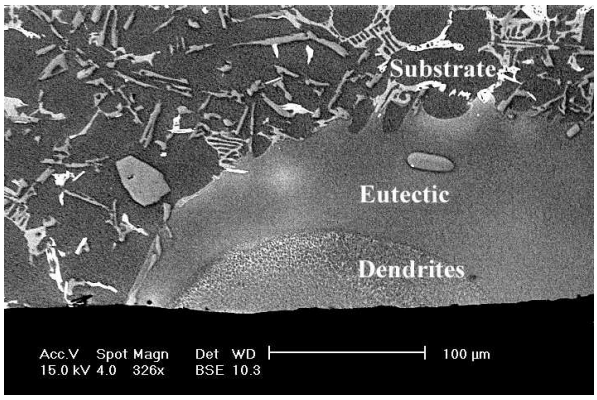

Fig.9 - SEM image of *Al-Si alloy* showing typical cross-sectional structure of an individual laser pulse; Condition: II-individual pulse.

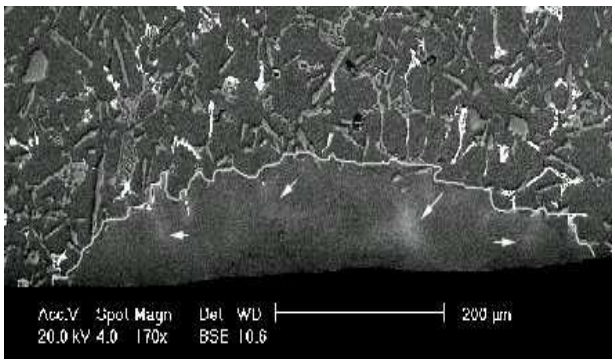

Fig.10 - SEM image of *Al-Si alloy* showing typical cross-sectional structure of an individual laser pulse; Condition III - individual pulse.

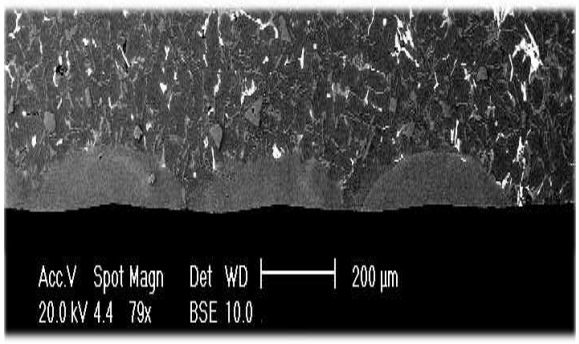

Fig.11 - SEM image of cross-section of *Al-Si alloy* sample with laser track; Condition II-track.

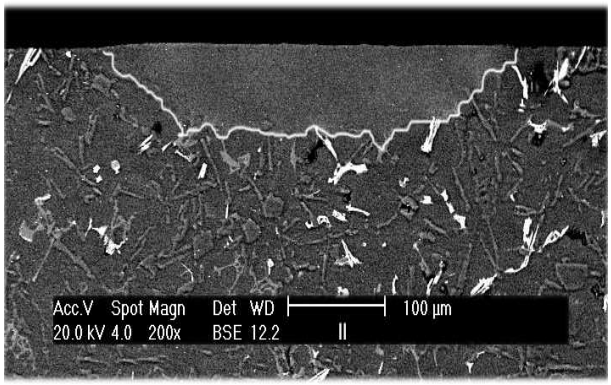

Fig.12 - SEM image of the *Al-Si alloy* (condition II).

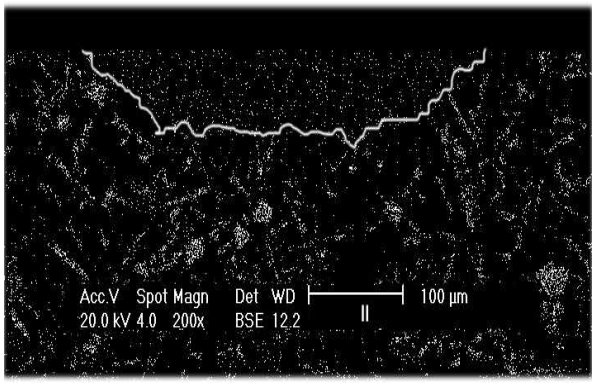

Fig.13 - X-ray mapping (SEM) of *Al-Si alloy* (condition II).

With EDS analysis, it was confirmed that with the laser treatment, there is an increase of the Si content in solution in the affected area. For completing this analysis, it was done an X-ray mapping where it was verified that for all conditions, the Si particles became smaller and more disperse in the matrix. The Figure 12 shows the SEM image of the microstructure in condition II, and the Figure 13 presents its respective X-ray mapping (SEM) image. With incidence of laser

tracks, it was obtained areas more uniform and homogeneous if compared with the incidence of individual pulses. However it was reached smaller maximum values of microhardness of 160 to 190HV, while for individual pulses it was reached maximum of 190 to 325HV.

Discussion and Conclusions

The effect of the gray iron laser treatment depends on the matrix microstructure changes, and the transformations depend on graphite lamellas solubilization process. The surface layer hardening due to martensite takes place mainly by transformation of pearlitic region of gray iron. The hardness values of martensite obtained depend on the austenization condition. Solubility differences between pearlitic iron carbide and lamellar graphite lead to very heterogeneous austenitizating conditions.
The laser surface hardening does not change the surface roughness and improves the material wear behaviour. On the other hand, laser surface melting leads to an increase in the roughness depending on the thickness of the molten layer.
The incidence of individual pulses or laser tracks using equal processing parameters, gives different microstructural aspect. It is due to the influence of the residual heat when laser tracks are applied. Parameters as scan velocity and overlapping are responsible for these microstructure modifications.
In all the tests a great increase of microhardness was verified. Depending on the selected laser treatment working conditions, different microstructures characteristics of surface hardening or surface melting can be achieved in the treated zone.
The increase of microhardness of the Al-Si alloy after laser heat treatment occurs due to the mechanism of dispersion hardening, a phenomenon like the precipitation hardening or aging, which only can be obtained in alloys that the solubility decrease with the cooling, i.e., when the solubility of phase rich in solute decreases. As the cooling rate of the laser treatment is very high, fine precipitates are formed improving the mechanical properties.
The high cooling rate causes the refinement of the Al-Si alloy structure, resulting in increase of microhardness due to the formation of solid solution of elementary silicon and eutectic particles. Depending on the selected laser treatment working conditions, different microstructures characteristics of surface melting can be achieved in the treated zone

References

[1] J. MAZUMDER, Laser Heat Treatment: The state of the art, J. Met., v.35, p.18, May, 1983.
[2] V.S. KOVALENCO; A.D. VERKHOTUROV; L.F. GOLOVKO; I.A. PODCHERNYAEVA, J. Sov. Laser Res., v.9, n.1, p. 46-58, 1988.
[3] BIROL, Y. *J. Mater. Sci.*, v.31, p.2139-2143, 1996.
[4] E.M.R. SILVA, W.A. MONTEIRO, J. VATAVUK, Acta Microscopica, v.8A, Proc. XVII Cong. of Brazilian Society for Microscopy and Microanalysis, Santos/SP, Oct., 1999, p. 345-346.
[5] E.M.R. SILVA, W.A. MONTEIRO, W. ROSSI, M.S.F. LIMA, J. Mater. Sci. Lett., v.19, n.23, p.2095-2097, Dec., 2000.

Acknowledgements

The authors would like to thank to UPM, CNPq and CAPES (Brazil) for financial support.

THERMEC 2009
doi:10.4028/www.scientific.net/MSF.638-642

Microstructural and Mechanical Characterization of Gray Cast Iron and AlSi Alloy after Laser Beam Hardening
doi:10.4028/www.scientific.net/MSF.638-642.769

References

[1] J. Mazumder, Laser Heat Treatment: The state of the art, J. Met., v.35, p.18, May, 1983.

[2] V.S. Kovalenco; A.D. Verkhoturov; L.F. Golovko; I.A. Podchernyaeva, J. Sov. Laser Res., v.9, n.1, p. 46-58, 1988.

[3] Birol, Y. J. Mater. Sci., v.31, p.2139-2143, 1996.
doi:10.1007/BF00356637

[4] E.M.R. Silva, W.A. Monteiro, J. Vatavuk, Acta Microscopica, v.8A, Proc. XVII Cong. of Brazilian Society for Microscopy and Microanalysis, Santos/SP, Oct., 1999, p. 345-346.

[5] E.M.R. Silva, W.A. Monteiro, W. Rossi, M.S.F. Lima, J. Mater. Sci. Lett., v.19, n.23, p.2095-2097, Dec., 2000.
doi:10.1023/A:1026750004296